

AN INDUCTIVE PICK-UP FOR BEAM POSITION AND CURRENT MEASUREMENTS

M. Gasior, CERN, Geneva, Switzerland

Abstract

An Inductive Pick-Up (IPU) senses the azimuthal distribution of the beam image current. Its construction is similar to a wall current monitor, but the pick-up inner wall is divided into electrodes, each of which forms the primary winding of a toroidal transformer. The beam image current component flowing along each electrode is transformed to a secondary winding, connected to a pick-up output. Four pick-up output signals drive an active hybrid circuit (AHC), producing one sum (Σ) signal, proportional to the beam current, and two difference (Δ) signals proportional also to the horizontal and vertical beam positions. The bandwidth of these signals ranges from below 1 kHz to beyond 150 MHz, exceeding five decades. Each electrode transformer has an additional turn to which a pulse from a precise current source is applied to calibrate the sensor for accurate beam position and current measurements. The IPU has been developed for the drive beam linac (DBL) of the Third CLIC Test Facility (CTF3) [1]. For that purpose it had to be optimized for low longitudinal coupling impedance in the GHz range.

CONSTRUCTION

The CTF3 DBL beam consists of a $1.5 \mu\text{s}$ train of 2.3 nC , $5 \text{ pS}_{\text{RMS}}$ electron bunches paced at a 1.5 GHz repetition rate [1], as shown in Figure 1. A position monitor for such a beam should have a low cut-off frequency in the kHz range to limit signal droops, a high cut-off frequency beyond 100 MHz to observe fast beam movements and longitudinal coupling impedance Z_C low in the GHz range, containing important beam frequency components, to limit the monitor influence on the beam. These requirements implied significant improvements over the LEP Pre-Injector pick-ups [2] on which this IPU design is based.

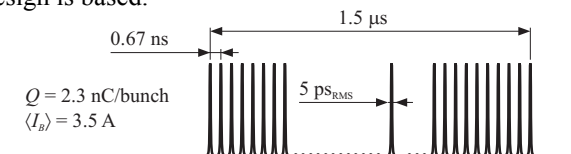


Figure 1: Time structure of the CTF3 DBL beam.

The IPU components and the assembly are shown in Figure 2 and 3 respectively. The 8 electrodes E have an internal diameter only 9 mm larger than the vacuum chamber of 40 mm and cover 75 % of the circumference in order to make the IPU as transparent to the beam as possible to minimize Z_C . The diameter step is occupied by the ceramic tube B of the vacuum assembly A; the tube is titanium coated on the inside. The electrodes are surrounded by the ferrite cylinder F inserted in the body C. The plates H accommodate the PCBs G on which the

transformers are mounted. A screw D passes through each transformer ring, connecting an electrode E to a plate H. The clamps I tighten the plates H with connectors screwed. To achieve good low frequency responses primary circuit parasitic resistances had to be kept below a $\text{m}\Omega$, thus the body C, the electrodes E and the plates H are made from copper. The plates as well as the beryllium copper screws D are gold plated. The electrodes and their supporting plate are machined as one piece to minimize contact resistances between small surfaces and to achieve good mechanical precision.

The four IPU outputs are connected to the AHC, which is followed by amplifiers housed in a common enclosure. The amplifiers, having two remotely switchable gains, amplify Δ and Σ signals to a level suitable to be sent over long cables to an equipment room.

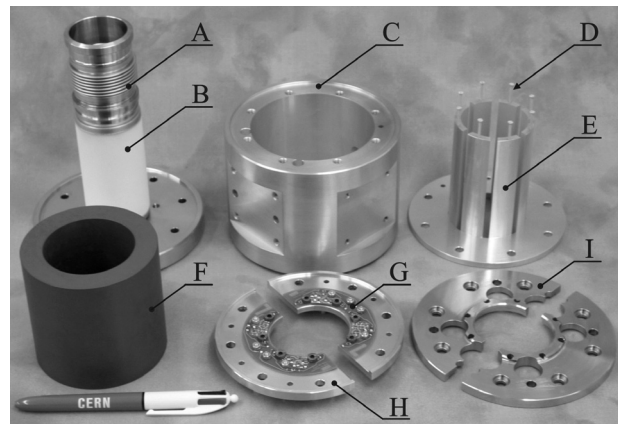


Figure 2: The IPU parts.



Figure 3: The IPU assembled. On the front there are four pick-up outputs and two calibration inputs.

The full beam image current must pass through the transformers, so the IPU can be used for its absolute measurement. To calibrate the sensor for this purpose, each transformer has a calibration turn, used to inject a current pulse of an amplitude known to 0.1 %, which in addition is independent of parasitic resistances of cables, connectors and the like. Similar pulses are used to test the Δ and Σ channels, calibrate their gains and check the common mode rejection ratio (CMRR) by applying identical signals to the transformers of opposite electrode pairs. This is important, since the AHCs are only one meter away from the beam and they are exposed to some radiation.

A MODEL AND RESULTS

The low frequency behavior of two opposite pairs of electrodes, forming one IPU plane, can be modeled by the circuit shown in Figure 4. Components of the beam image current I_B flow through four 1: n electrode transformers, which are combined in pairs so that each sees half of the secondary winding load R_S . The output Σ signal voltage

$$V_\Sigma = \frac{R_S}{2n} I_B \quad (1)$$

decays with the time constant set by $R_p = R_S / 2n^2$, representing R_S transformed to the primary winding, and inductance L_Σ of the loops built from electrodes and the body walls; the loops are filled with the ferrite. Taking into account parasitic connection resistances R_C of primary loops yields the Σ signal low cut-off frequency

$$f_{L\Sigma} = \frac{1}{2\pi L_\Sigma} \left(\frac{R_S}{2n^2} + R_C \right) \quad (2)$$

provided that the transformer low cut-off is still smaller.

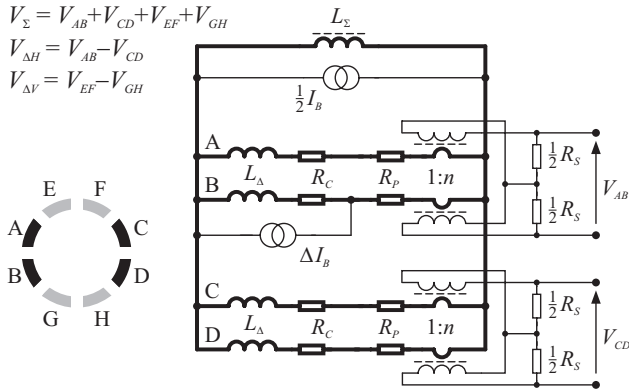


Figure 4: IPU low frequency model for one plane.

Similarly, the current ΔI_B resulting from the beam displacement decays with the time constant set by the sum $R_p + R_C$ and electrode inductance L_A . The corresponding low cut-off frequency is

$$f_{L\Delta} = \frac{1}{2\pi L_A} \left(\frac{R_S}{2n^2} + R_C \right) \quad (3)$$

The number of turns n was a trade-off between four parameters: the low cut-off frequencies $f_{L\Sigma}$ and $f_{L\Delta}$ proportional to n^2 , the voltage V_Σ changing as n^{-1} and

high cut-off frequencies, degrading with increasing n . The low cut-off frequencies were also reduced by lowering R_S at the expense of decreasing V_Σ . Since $L_A \ll L_\Sigma$ resulting in $f_{L\Delta} \gg f_{L\Sigma}$, only frequency $f_{L\Delta}$ was lowered by another decade using extra low frequency gain in the Δ signal amplifier. Parameters of the model of Figure 4, the IPU and a channel IPU-AHC are listed in Table 1.

Table 1. Parameters of the IPU and of its electronics.

IPU	Electrical centre position error	< 0.1 mm
	Range of linearity to 50 μm	± 5 mm
	Transformer load R_S / turn number n	7 Ω / 30
	L_Σ / L_A inductances / ferrite μ_r	≈ 5 μH / 70 nH / 100
	Primary winding resistance R_p	4 m Ω
	Primary parasitic resistance R_C	≈ 0.5 m Ω
	Transresistance V_Σ / I_B	0.1 Ω
	IPU electrode high cut-off frequency	300 MHz
	IPU Σ low cut-off frequency	150 Hz
	IPU Δ low cut-off (without the slope)	10 kHz
	Titanium coating end-to-end resistance	10 Ω (i.e. 15 Ω / \square)
	Coupling imp. Z_C @ 1.5 / 3 GHz	9 + j2 / 10 - j0.5 Ω
Beam pipe / electrode inner diameter	40 mm / 49 mm	
Length with bellows / body diameter	168 mm / 130 mm	
IPU + AHC	Position sensitivity	10 mm $\times \Delta \Sigma$
	Overall Σ signal bandwidth	300 Hz - 250 MHz
	Overall Δ bandwidth (without slope)	800 Hz - 150 MHz
	Δ equivalent noise @ $\langle I_B \rangle$ 3A / 0.3A	< 5 μm_{RMS} / < 50 μm_{RMS}
	Σ equivalent noise, low / high gain	< 3 mA $_{\text{RMS}}$ / < 3 mA $_{\text{RMS}}$
	Σ signal amplifier gain low / high	5 / 25 dB
	Δ signal amplifier gain low / high	15 / 35 dB
AHC CMRR @ 1 / 100 MHz	> 60 dB / > 50 dB	
Calibration current pulse	300 mA 0.1 %, 150 μs	

The transformer load R_S is as small as 7 Ω making the secondary winding circuit very sensitive to parasitic series inductances. To minimize them, R_S is built from 6 chip resistors and connections between components of the secondary winding are made by sections of low impedance microstrip lines.

Frequency characteristics of the IPU with the AHC are plotted in Figure 5. The measurement was done with a wire method, where beam is simulated by the central conductor of a coaxial line which the IPU was a part. The Σ signal is flat to 0.5 dB over 5 decades. The Δ signal, originating in a small central conductor displacement, has a 3 dB slope for some 4 decades, which can be explained by a frequency dependence of the ferrite permeability and electrode current surface distribution.

The PCB layout of the AHC module was carefully designed to obtain sufficient CMRR at high frequencies. Note that the achieved CMRR of better than 50 dB at 100 MHz is equivalent to 0.1 pF of parasitic asymmetry of a 50 Ω line.

The IPU displacement characteristic is linear to 50 μm for excursions up to ± 5 mm, most important for the DBL. The linearity error, shown in Figure 6, was measured with the wire method, where a thin wire was displaced diagonally through the pick-up aperture.

The IPU longitudinal coupling impedance Z_C was estimated by a wire method measurement shown in Figure 7. It can be seen that the components beyond

1 GHz flow essentially only over the titanium coating, so its resistance of about 10Ω limits the Z_C , hopefully also beyond 3 GHz. Above this frequency waveguide modes were observed in the setup and the measurement did not yield meaningful data.

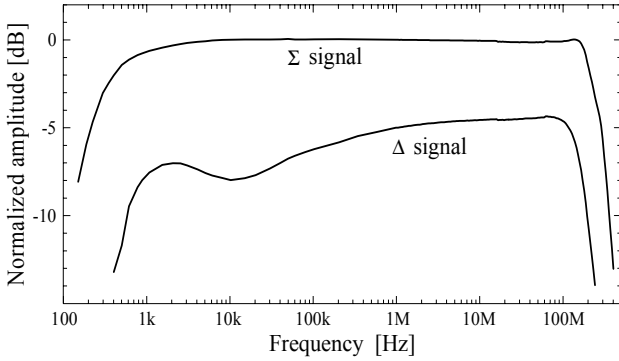


Figure 5: Characteristics of the IPU with its AHC. Measured with a 50Ω coaxial line setup (wire method).

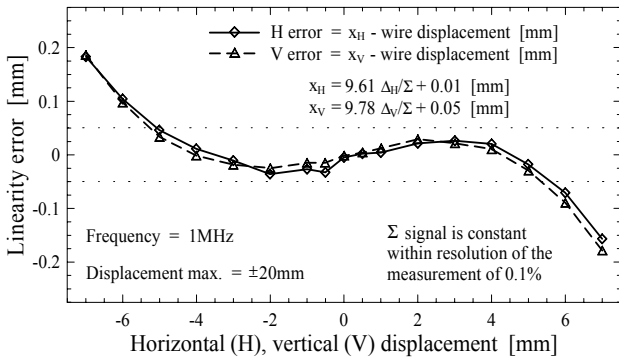


Figure 6: IPU linearity error. Measured with a wire of diameter of 0.2 mm displaced diagonally.

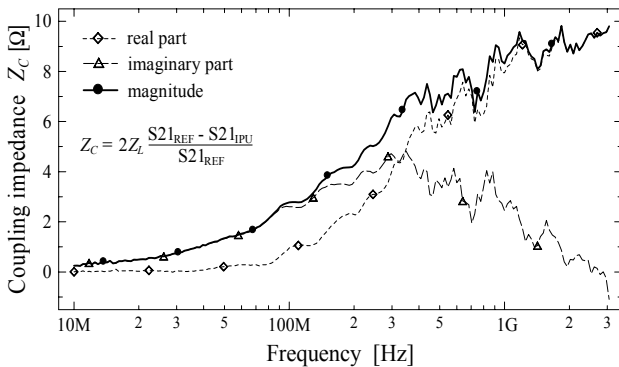


Figure 7: Longitudinal coupling impedance Z_C measured with a coaxial setup of $Z_L = 50 \Omega$ (wire method). For the $S21_{REF}$ reference measurement the IPU was replaced by an equivalent length of a straight tube.

The IPU influence for the beam may also be deduced from a Time Domain Reflectometry (TDR) measurement shown in Figure 8. For high frequency components the electrode diameter step is not visible, as they flow over the coating. For lower frequencies an impedance increase

of about 6Ω is seen, corresponding to the electrode diameter step for the most part occupied by the ceramic insertion (alumina, $\epsilon_r \approx 10$).

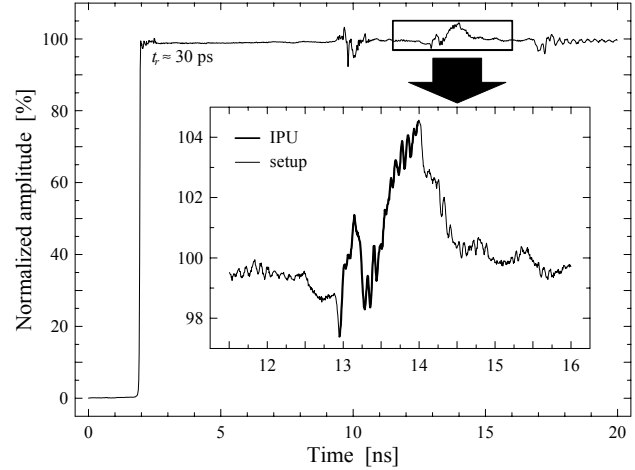


Figure 8: IPU TDR measurement with a 50Ω coaxial setup (wire method) and TDR module Agilent 54753A. Ripples in the magnified region originate in setup waveguide modes and the irregularities outside the region result from setup imperfections, especially of the conical adaptations.

CONCLUSIONS AND THE FUTURE

An inductive pick-up and a dedicated active hybrid circuit were designed for the drive beam linac of the CTF3. They allow to measure beam position with a bandwidth of 5 decades and absolute beam current over 6 decades. The IPU with its AHC can be tested and calibrated in place with precise current pulses. Neither the IPU nor the AHC contain adjustable elements. The pick-up longitudinal impedance was limited to about 10Ω in the GHz range. The pair IPU-AHC has been tested with a beam in the CTF2. Two monitors have been installed in the CTF3 for the startup in June. An acquisition system [3] based on 12-bit fast digitizers is being developed. In the future some 20 IPU's will be installed in the facility.

ACKNOWLEDGMENTS

I would like to thank all members of my AB/BDI/PI section for their help, especially to J. Belleman, J. Durand, J.L. Gonzalez, J.P. Potier and L. Søby. I am also grateful to Y. Cuvet for the superb mechanical design and to J.L. Chauvet for excellent PCBs.

REFERENCES

- [1] G. Geschonke et al., "CTF3 Design Report", CTF3 Note 047, CERN, May 2002.
- [2] S. Battisti et al., "Magnetic Beam Position Monitors for LEP Pre-Injector", Proceedings of the 1987 IEEE PAC, Washington, March 16-19 1987, pp. 605 – 607.
- [3] M. Gasior, "Hardware of the CTF3 Beam Position Measurement System", CTF3 Note 053, CERN, February 2003.